Journal of Solid State Chemistry 183 (2010) 1582–1587

Contents lists available at ScienceDirect

Journal of Solid State Chemistry

journal homepage: www.elsevier.com/locate/jssc

Hydrothermal synthesis, characterization and composition-dependent magnetic properties of $LaFe_{1-x}Cr_xO_3$ system ($0 \le x \le 1$)

Weiwei Hu, Yan Chen, Hongming Yuan, Ganghua Zhang, Guanghua Li, Guangsheng Pang, Shouhua Feng*

State Key Laboratory of Inorganic Synthesis and Preparative Chemistry, College of Chemistry, Jilin University, Changchun 130012, PR China

ARTICLE INFO

Article history:
Received 26 November 2009
Received in revised form
20 April 2010
Accepted 30 April 2010
Available online 5 May 2010

Keywords:
Hydrothermal synthesis
Perovskites
Magnetic property
Superexchange interaction

ABSTRACT

Hydrothermal synthesis, characterization and magnetic properties of a series of ABO_3-perovskites $LaFe_{1-x}Cr_xO_3$ ($0 \le x \le 1$) are reported. The alkalinity in initial reaction mixtures plays a critical role in controlling the designed stoichiometry of the final compositions. Their magnetic properties are strongly dependent on the compositions and a maximum magnetic moment is found for the sample at $x=0.5$. Weak ferromagnetic interaction observed for the samples from $x=0$ to 0.9 arises from the presence of Fe–O–Fe antisymmetric exchange and Fe–O–Cr superexchange interaction. The weak ferromagnetism as well as the linear variation of the lattice parameters implies the possible random distribution of Fe and Cr ions in B sites of the perovskites. The evolution of magnetic ordering transition temperatures has a close relationship with substituent ratios, for the competition of antiferromagnetism and ferromagnetism. The saturated magnetic moment shows a great improvement compared with that for the samples synthesized by solid state method.

1. Introduction

Colossal magnetoresistance and multiferroic materials and their applications to memory and sensing devices have promoted enormous interests in finding new functional materials with a large coupling between magnetism and electronic conductivity or electrical polarization [1–3]. The design for the materials with a large ferromagnetic ordering is still a challenge. Previous studies on Cr-doped rear earth (Re) ferrites, $ReFe_{1-x}Cr_xO_3$ with ABO_3-perovskite structures have predicted their possible strong ferromagnetic (FM) coupling [4,5]. According to the Kanamori–Goodenough (KG) rule, Fe(d_5)–O–Cr(d_3) would show FM behavior through superexchange interaction when Fe and Cr were arranged orderly at B sites [6,7]. Miura and Terakura [4] performed band-structure calculations based on the generalized gradient approximation and the local-density approximation plus U method, and confirmed the ground state of ordered $LaFe_{0.5}Cr_{0.5}O_3$ to be ferromagnetism. However, no saturated magnetic moment was observed experimentally, for Fe and Cr ions were randomly distributed at B sites in bulk samples [8]. Mössbauer spectrum [9] was explored to investigate the substitution of Cr for Fe in $LaFeO_3$ and the magnetic properties are closely related to the Cr doping level, and antiferromagnetic (AFM) interaction is dominated. Similar effect was found in $ReFe_{1-x}Cr_xO_3$ (Re=Y or Nd) systems [10,11]. Suchomel et al. [12] prepared the room temperature multiferroic solid $BiFe_{0.5}Cr_{0.5}O_3$ at high pressure, but it is still AFM, even though FM and ferroelectric Bi_2NiMnO_6 were synthesized by a similar process [13]. So far, FM spin order was only found in $LaCrO_3$–$LaFeO_3$ superlattice, artificially created by laser molecular beam epitaxy, where layered CrO and FeO were stacked alternately along the [111] direction [14].

At present, studies on $ReFe_{1-x}Cr_xO_3$ system were focused mainly on the theoretical calculation. Probably due to the limitation of the prepared method, few experiments were performed to investigate the dependence of magnetic properties on the compositions with various Cr-doped levels. In this study, we employed mild hydrothermal method to synthesize our samples at relatively low temperature. This method allows one-pot liquid synthesis and doping, and products are usually pure phases [15–17]. Our motivation is to prepare a whole series of $LaFe_{1-x}Cr_xO_3$ ($0 \le x \le 1$) and check whether B-site ordering compositions can be formed according to the liquid nucleation mechanism of hydrothermal reactions, different from the diffusion mechanism of solid state reactions. In addition, the precious control of initial reaction conditions gave designed stoichiometric compositions of solids, which is obviously important for the comparison investigation of magnetic properties.

2. Experimental section

The hydrothermal synthesis of $LaFe_{1-x}Cr_xO_3$ was carried out in 18-mL Teflon-lined stainless steel autoclave with a filling capacity of 80%. Solutions of 0.4 M $La(NO_3)_3$, 0.4 M $CrCl_3$ and 0.4 M

* Corresponding author. Fax: +86 431 85168624.
E-mail address: shfeng@jlu.edu.cn (S. Feng).

0022-4596/$ - see front matter © 2010 Elsevier Inc. All rights reserved.
doi:10.1016/j.jssc.2010.04.041

$Fe(NO_3)_3$ were prepared in advance before synthesis. In a typical synthetic procedure of $LaFe_{0.5}Cr_{0.5}O_3$, 1 g KOH were added to 2.5 mL $CrCl_3$ and 2.5 mL $Fe(NO_3)_3$ to get a suspension. 5 mL $La(NO_3)_3$ and 4 g KOH were then added in sequence on vigorous stirring for 10 min to form a mixture. The mixture was transferred into the autoclave and heated at 513 K for 5 days. The Dark red powder product was filtered and washed with deionized water. Similar procedures were applied to other compositions by adjusting the initial Fe/Cr ratios and KOH contents according to their initial reaction compositions. Product compositions were determined by inductively coupled plasma spectroscopy (ICP) as well as energy dispersive spectroscopy (EDS).

Powder X-ray diffraction (XRD) data were collected on a Rigaku D/Max 2500 V/PC X-ray diffractometer with Cu$K\alpha$ radiation ($\lambda = 1.5418$ Å) at 40 kV and 200 mA at room temperature. The step scanning in the angle range of $20^\circ \le 2\theta \le 80^\circ$ and increments of 0.02° were employed. Pawley refinement was performed with Accelrys MS Modeling software. Scanning electron microscope (SEM) images were taken with a JEOL JSM-6700F microscope operating at 10 kV. Hysteresis, zero-field-cooled (ZFC) and field-cooled (FC) magnetization measurements were performed on a SQUID magnetometer.

3. Results and discussion

All samples were characterized by room temperature powder XRD and Pawley refinements were conducted. Fig. 1 shows XRD patterns and Pawley refinements for selected samples of $x = 0.2$, 0.5, and 0.8 (other samples' XRD patterns are given in Fig. S1). Compositional analyses by ICP and EDS gave a formula of $LaFe_{1-x}Cr_xO_3$ ($0 \le x \le 1$). (EDS results for $x = 0.2$, 0.4, 0.5, 0.6, and 0.8 samples are illustrated in Fig. S2.) All XRD peaks could be indexed in orthorhombic system with space group *Pnma*. The lattice parameters refined by the Pawley method are listed in Table 1 and the variation of unit cell parameters with Cr content (x) of $LaFe_{1-x}Cr_xO_3$ is shown in Fig. 2. As seen in Table 1 and Fig. 2, the lattice parameters of $LaFeO_3$ and $LaCrO_3$ are consistent with previously reported values [18,19]. The unit cell parameters a, b, c and volume V gradually decrease with increasing Cr content. Such a monotonous decrease is associated with the incorporation of smaller Cr ion (0.615 Å) into the site of Fe ion (0.645 Å) where Fe (III) is at high-spin state [11]. The facts of pure phase and graduate lattice decrease imply the incorporation of Cr^{3+} ions into B sites of the perovskites.

KOH as a mineralizer plays an important role in forming the perovskites and changing Fe/Cr ratios of products. The mineralizing effect was also seen in the hydrothermal synthesis of other complex transition metal oxides [20–22]. In this work, we particularly found that the final compositions were strongly dependent on alkalinity in initial reactant mixture. The product Fe/Cr ratio increases with the initial reactant alkalinity. For example, in the synthesis of $LaFe_{0.5}Cr_{0.5}O_3$ we may start with an expecting Fe/Cr = 0.5:0.5 and an optimum alkalinity [KOH] = 9 M in the initial composition. When [KOH] deviated from the optimum value appreciably, such as 10, 11.4, 12.8, 14.3 and 15.6 M, the final products are $LaFe_{0.56}Cr_{0.44}O_3$, $LaFe_{0.60}Cr_{0.40}O_3$, $LaFe_{0.80}Cr_{0.20}O_3$, $LaFe_{0.95}Cr_{0.05}O_3$ and $LaFeO_3$, respectively. Similar effect was found in the synthesis of $LaFe_{0.7}Cr_{0.3}O_3$. When we fixed the Fe/Cr = 0.7:0.3, the amounts of KOH of 3, 6 and 9 M corresponded to the final products of $LaFe_{0.70}Cr_{0.30}O_3$, $LaFe_{0.75}Cr_{0.25}O_3$ and $LaFe_{0.80}Cr_{0.20}O_3$, respectively. Our synthesis was monitored by composition and XRD analysis. It seems that any ratio product in the system $LaFe_{1-x}Cr_xO_3$ could be synthesized by controlling the alkalinity, regardless of yield. The effect of alkalinity can be explained by oxidation of Cr species in solution [19]. We think the mechanism is complicated; it involves not only oxidation but also condensation, which is more or less related to the coordinate states of metal ions at a given alkalinity. However, the present results indicated the possible precious control of a designed composition by alkalinity.

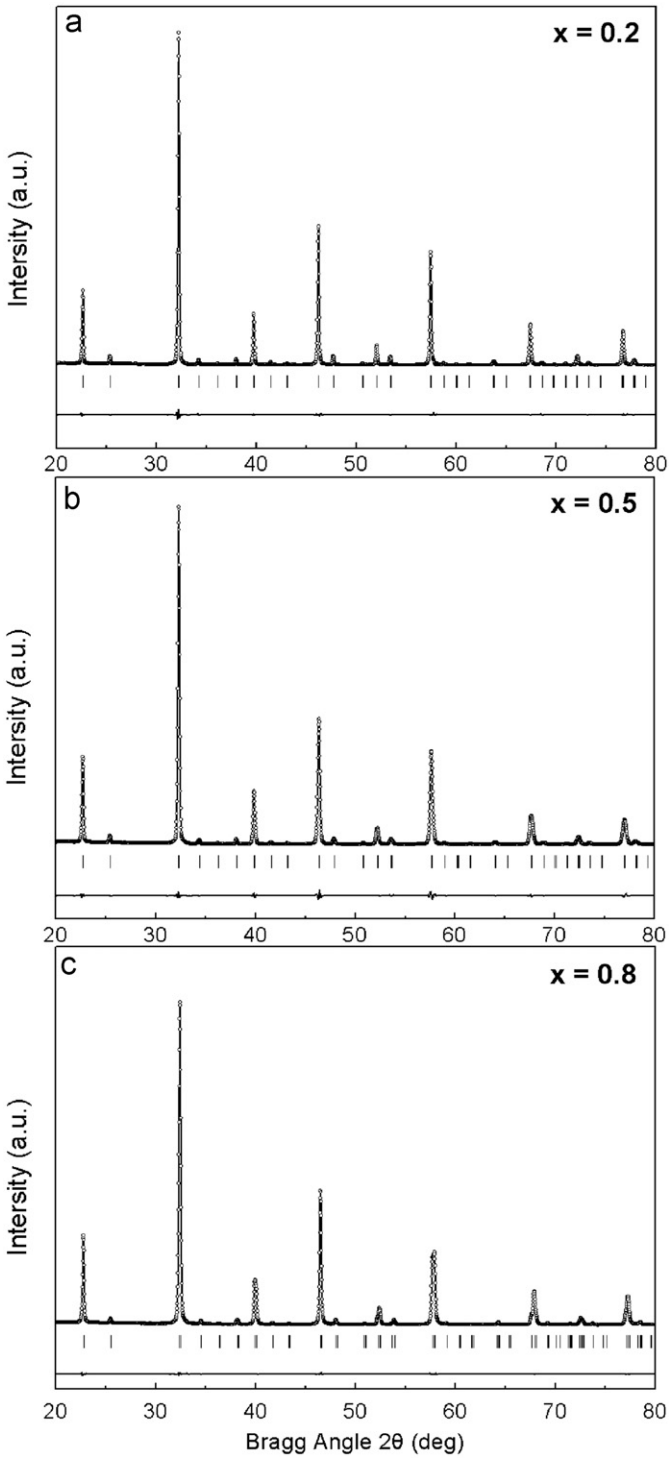

Fig. 1. Pawley refinement of samples (a) $x = 0.2$, (b) $x = 0.5$ and (c) $x = 0.8$ from XRD data. All peaks can be well indexed in orthorhombic *Pnma*. Observed (○), calculated (line), and difference (bottom) profiles are shown. The Bragg reflection positions are marked with vertical bars.

Fig. 3 shows SEM images of $LaFe_{1-x}Cr_xO_3$. All the products are cubic shaped powder crystals with sizes ranging from 1 to 13 μm in accordance with those results for previously hydrothermally synthesized $LaCrO_3$ [19] and $LaFeO_3$ [23].

The temperature dependence of magnetization was measured at 0.1 T for $LaFe_{1-x}Cr_xO_3$. As shown in Fig. 4, the magnetization strongly depended on the composition. The magnetic moment at 4 K increased from 0.057 emu/g for $x=0$ up to the maximum value of 2.55 emu/g for $x=0.5$, and then decreased to the minimum value of 0.030 emu/g for $x=1.0$. The small peak at $T\sim 50$ K may originate from little oxygen leakage from the equipment [24], since they have almost the same value of ~ 0.002 emu/g above the curve. The hysteresis loops from the isothermal magnetization curves at 4 K for $x=0$–0.9 indicated the presence of FM behavior, as shown in Fig. 5. However, none reached the saturation up to 5 T, indicating a weak FM interaction, which arises from the coexistence of the Fe–O–Cr FM superexchange interaction and Fe–O–Fe or Cr–O–Cr AFM interaction.

Table 1
The unit cell parameters of $LaFe_{1-x}Cr_xO_3$ (space group *Pnma*).

x	a (Å)	b (Å)	c (Å)	V (Å^3)	R_{wp} (%)	R_p (%)
0	5.5566(3)	7.8555(5)	5.5653(4)	242.92	7.76	4.47
0.1	5.5557(1)	7.8541(1)	5.5638(1)	242.77	5.41	3.30
0.2	5.5514(1)	7.8482(1)	5.5577(2)	242.14	5.62	2.91
0.3	5.5413(1)	7.8383(2)	5.5563(4)	241.33	7.96	5.39
0.4	5.5351(2)	7.8315(3)	5.5462(4)	240.42	5.10	3.49
0.5	5.5287(2)	7.8175(3)	5.5373(2)	239.32	4.86	3.35
0.6	5.5190(0)	7.8110(1)	5.5363(0)	238.66	3.71	2.29
0.7	5.5130(1)	7.8017(1)	5.5341(1)	238.02	4.66	3.01
0.8	5.5036(0)	7.7914(1)	5.5333(0)	237.27	3.36	1.96
0.9	5.4987(1)	7.7869(1)	5.5291(1)	236.74	3.83	2.48
1.0	5.4870(1)	7.7742(1)	5.5248(1)	235.66	4.54	3.17

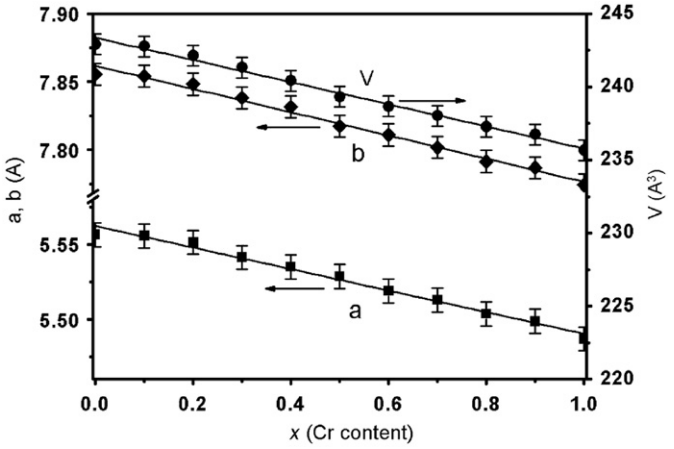

Fig. 2. The unit cell parameters a, b and volume V vs. x (Cr content) of $LaFe_{1-x}Cr_xO_3$.

The maximum magnetization (M_{max}) (at $T=4$ K and $H=5$ T) and remnant magnetization (M_r) from isothermal magnetization curves showed the same tendency as magnetization versus temperature, as shown in Fig. 6. Both of them increased first and reached a maximum at $x=0.5$ with $M_{max}=5.73$ emu/g and $M_r=1.74$ emu/g, and then decreased to almost zero at $x=1.0$. This symmetric trend was formed by the substitution of Cr ion for Fe ion, which entered into the lattice of $LaFeO_3$. $LaFeO_3$ is AFM due to Fe–O–Fe exchange interaction. Very weak ferromagnetism of $LaFeO_3$, as seen in hysteresis loop, ascribed from the spin canting due to antisymmetric exchange [25]. As Cr ions are incorporated into the B-site, three exchange interactions may be present due to the random distribution of the B-site cations: Fe–O–Fe, Fe–O–Cr and Cr–O–Cr. As we know that Fe–O–Fe and Cr–O–Cr are AFM interaction, whereas Fe–O–Cr superexchange interaction shows FM interaction, which will enhance the magnetization. With the increase of Cr content, the proportion of Fe–O–Cr interaction increased, leading to the formation of inhomogeneous distribution of FM clusters in the lattice, and reached a maximum at $x=0.5$, as seen in Fig. 6. Further incorporation of Cr may increase the proportion of Cr–O–Cr AFM interaction, and thus the magnetization starts to decrease. Until down to $LaCrO_3$, only Cr–O–Cr AFM interaction exists.

This symmetric trend was quite different from a previous report [9], where the samples were prepared by self-propagating high-temperature method. For those samples the peaks of M_{max} and M_r were at $x(Cr)=0.25$. In our work the peaks were at $x=0.5$ and the magnitudes were much higher. Our result is consistent with theoretical prediction that $LaFe_{0.5}Cr_{0.5}O_3$ should show the

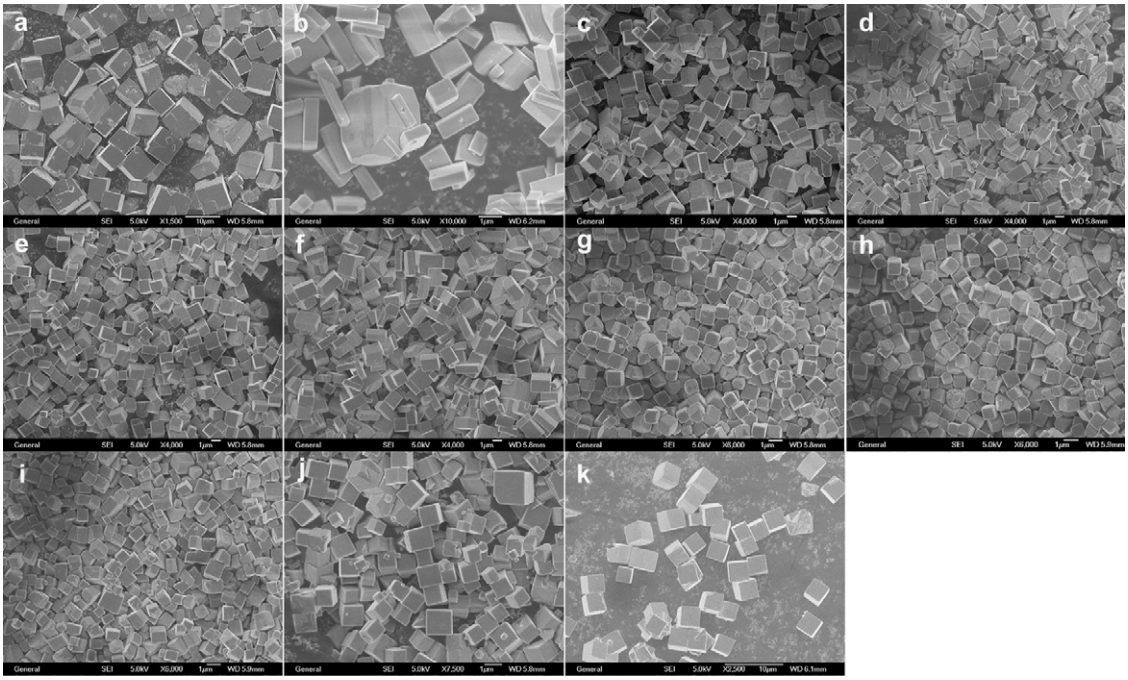

Fig. 3. SEM images of $LaFe_{1-x}Cr_xO_3$: (a) $x=0$; (b) $x=0.1$; (c) $x=0.2$; (d) $x=0.3$; (e) $x=0.4$; (f) $x=0.5$; (g) $x=0.6$; (h) $x=0.7$; (i) $x=0.8$; (j) $x=0.9$; (k) $x=1.0$.

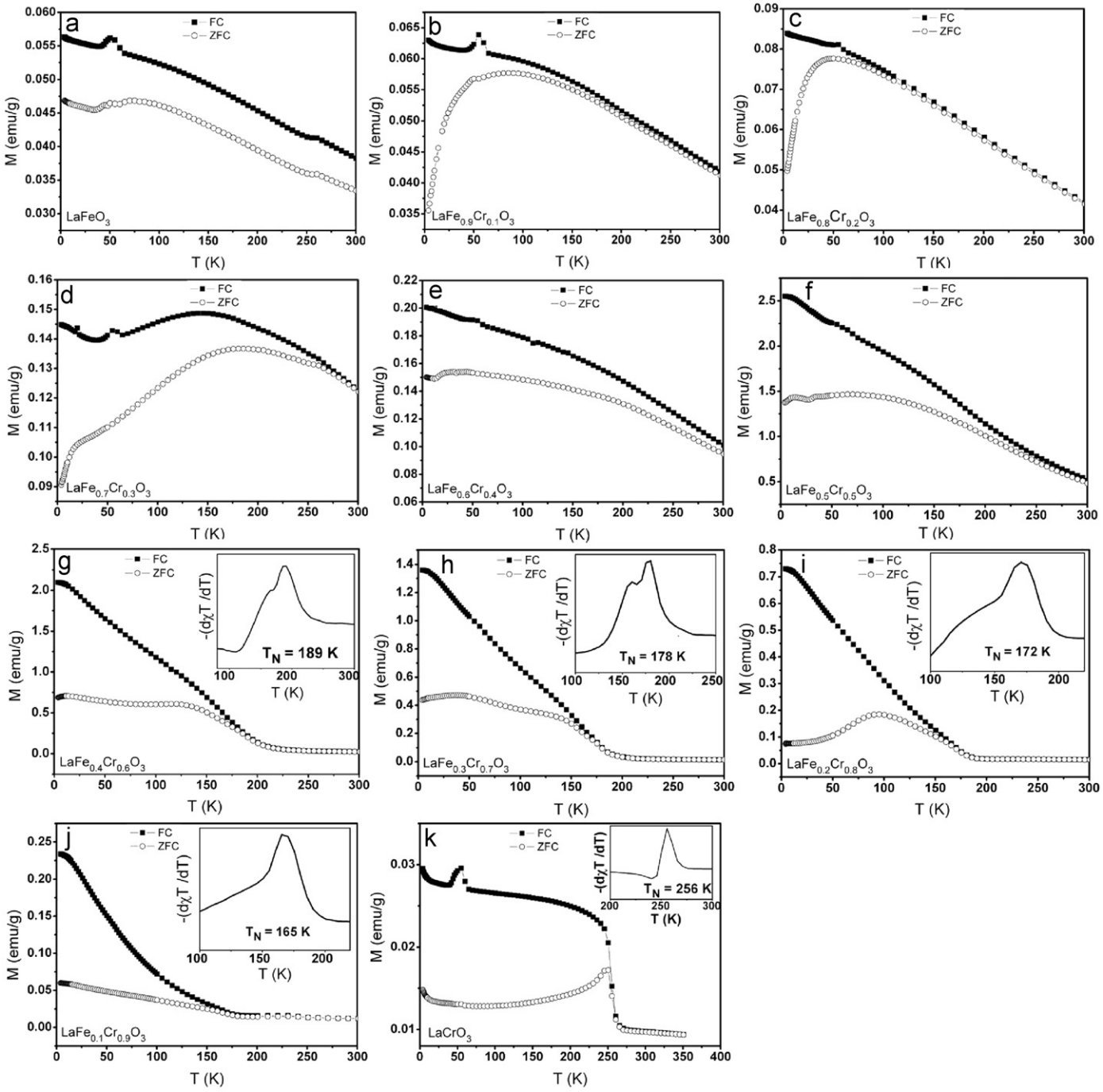

Fig. 4. Temperature dependence of magnetization (ZFC and FC) of $LaFe_{1-x}Cr_xO_3$ at 0.1 T: (a) $x=0$; (b) $x=0.1$; (c) $x=0.2$; (d) $x=0.3$; (e) $x=0.4$; (f) $x=0.5$; (g) $x=0.6$; (h) $x=0.7$; (i) $x=0.8$; (j) $x=0.9$; (k) $x=1.0$. The inset of (g)–(k) shows the derivation of $-\chi T$ vs. T curves.

most significant superexchange interaction of Fe–O–Cr, having the largest magnetic moment. According to the KG rule [6,7] and theoretical calculation by Miura and Terakura [4], combined Fe–O–Cr linkages in $LaFe_{0.5}Cr_{0.5}O_3$ would show FM behavior through superexchange interaction when Fe and Cr ions were arranged orderly in B sites. However, no saturated magnetic moment was found at $x=0.5$ in our work, due to the mixed distribution of Fe–O–Fe, Fe–O–Cr and Cr–O–Cr exchange interactions. The lattice parameters vary linearly as a function of Cr content, in accordance with Vegard's law, also indicating the possible random distribution of Fe and Cr in B sites as shown in Fig. 2. The saturated magnetization (M_s) was extrapolated to be $0.21\mu_B$/f.u. for $LaFe_{0.5}Cr_{0.5}O_3$, as seen in the inset of Fig. 5(b). According to a theoretical estimation, a total magnetization value of $4\mu_B$ would be expected, corresponding to high-spin states for both Fe and Cr and an FM ordering of all spins [5]. Although our sample's M_s is far from the theoretical value, it is much larger than any previously reported value [10–12]. Azad et al. [26] presented a saturated value of $0.04\mu_B$/f.u. for the sample prepared by solid state sintering method. Our result revealed that an increased Fe–O–Cr FM ordering could be created in the samples from hydrothermal systems.

The compositional dependence of magnetic transition temperature was observed for samples of $x=0.6$–1.0, as shown in Fig. 7. For the samples of $0 \le x \le 0.5$, transition temperatures were beyond the measurable range of SQUID, but the M–T curves in Fig. 4 indicated that they also followed a falling trend. At $x=0$, $LaFeO_3$ showed a

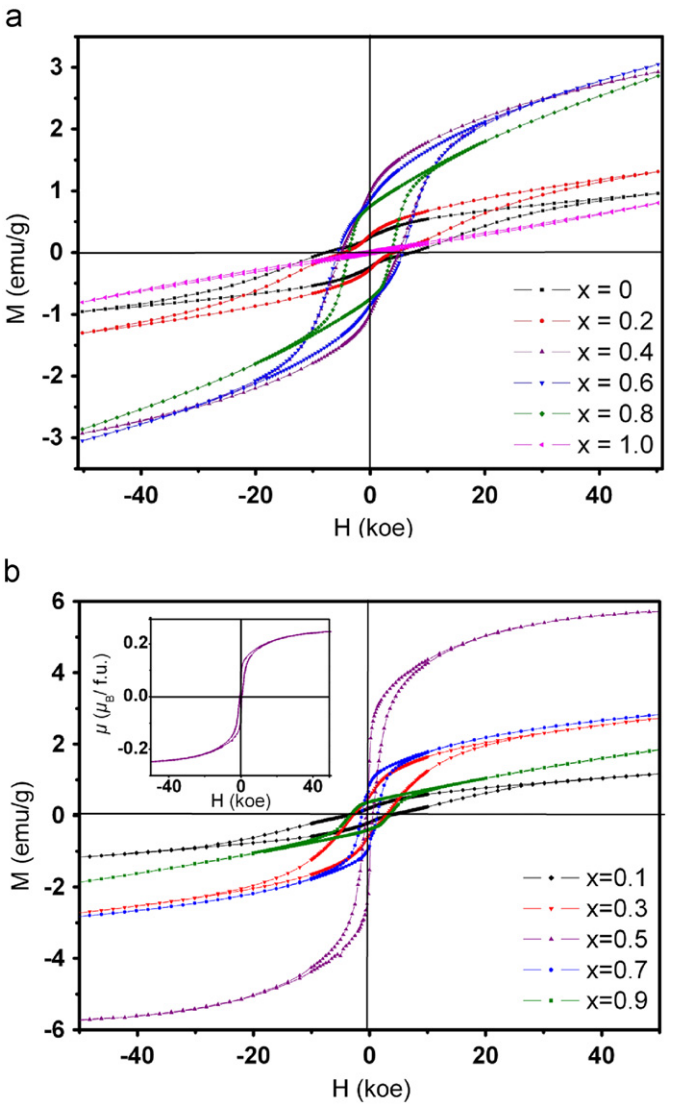

Fig. 5. Isothermal magnetization curves for $LaFe_{1-x}Cr_xO_3$ at 4 K: (a) even compositions and (b) odd compositions. The inset of (b) shows the saturated magnetic moment of $LaFe_{0.5}Cr_{0.5}O_3$ per formula unit.

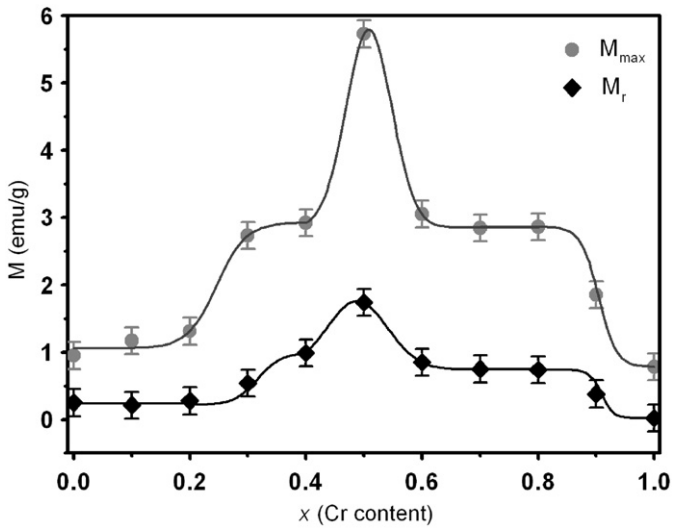

Fig. 6. The maximum magnetization (M_{max}) (upper) and remnant magnetization (M_r) (lower) as a function of x (Cr content). Both curves followed a similar symmetric trend and reached a peak at $x=0.5$, with $M_{max}=5.73$ emu/g and $M_r=1.74$ emu/g.

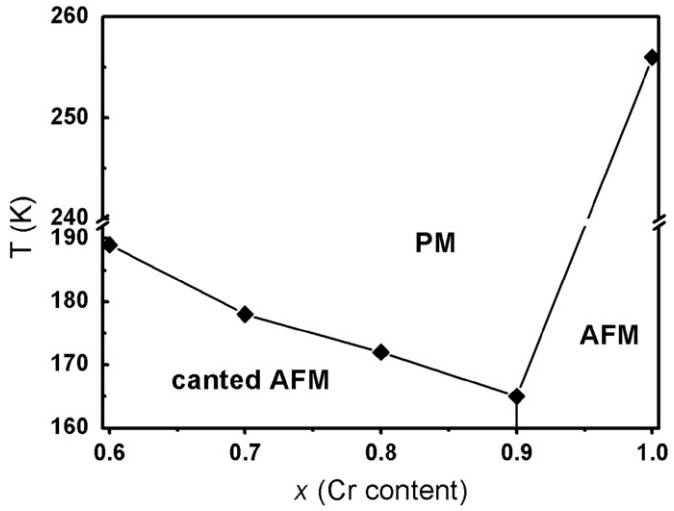

Fig. 7. The evolution of magnetic transition temperature with various Cr content. For $0 \le x \le 0.5$, the transition temperatures were beyond the allowed range of SQUID.

well-known AFM behavior with $T_N=740$ K [18]. The introduction of Cr increased the probability of Fe–O–Cr superexchange interaction and formation of FM clusters. The magnetic transition temperature decreased due to the presence of Fe–O–Cr FM interaction, as observed in $LaMn_{0.85}Cr_{0.15}O_{3+\delta}$ with various oxygen contents [27]. The magnetic ordering transition temperature shows a minimum value at $x=0.9$, where FM phase still presented in this region. Above $x=0.9$, the AFM transition temperature increased up to 256 K for $LaCrO_3$, due to the overwhelming AFM interaction of Cr–O–Cr. This value is smaller than other literature values of ~290 K for $LaCrO_3$ prepared from the solid state method [18]. This is possibly correlated with local structural change and oxygen-rich surface of hydrothermal samples [28]. It is the characteristic of hydrothermal reaction, e.g., producing expanded cell and more hydroxyl groups on the surface of samples [19].

4. Conclusions

A whole series of compounds $LaFe_{1-x}Cr_xO_3$ $(0 \le x \le 1)$ was synthesized by mild hydrothermal method. Hydrothermal reaction is suitable to form well-crystallized products and alkalinity of initial reactant composition is a critical factor to control preciously the Fe/Cr ratios of final products. The substitution of Cr ions for Fe ions affects the relative proportion of Fe–O–Cr ferromagnetic superexchange interaction, and thus results in a symmetric change of magnetic measurement with maximum at $x=0.5$. The frustration of antiferromagnetism and ferromagnetism leads to the decrease of magnetic ordering transition temperature. Despite Fe^{3+} and Cr^{3+} ions being distributed randomly in the B-site, an enhanced saturated magnetic moment of $0.21\mu_B$/f.u. was obtained for the sample with $x=0.5$. Our results indicate that the hydrothermal synthetic approach can be applied to prepare magnetic ordering materials.

Acknowledgment

We thank the National Nature Science Foundation of China for financial support of this work.

Appendix A. Supplementary Material

Supplementary data associated with this article can be found in the online version at doi:10.1016/j.jssc.2010.04.041.

References

[1] M. Uehara, S. Mori, C.H. Chen, S.-W. Cheong, Nature 399 (1999) 560–563.
[2] S.-W. Cheong, M. Mostovoy, Nat. Mater. 6 (2007) 13–20.
[3] K.F. Wang, J.-M. Liu, Z.F. Ren, Adv. Phys. 58 (2009) 321–448.
[4] K. Miura, K. Terakura, Phys. Rev. B 63 (2001) 104402.
[5] P. Baettig, C. Ederer, N.A. Spaldin, Phys. Rev. B 72 (2005) 214105.
[6] J. Kanamori, J. Phys. Chem. Solids 10 (1959) 87–98.
[7] J.B. Goodenough, Phys. Rev. 100 (1955) 564–573.
[8] A. Wold, W. Croft, J. Phys. Chem. 63 (1959) 447–448.
[9] M.V. Kuznetsov, Q.A. Pankhurst, I.P. Parkinc, Y.G. Morozov, J. Mater. Chem. 11 (2001) 854–858.
[10] A. Dahmani, M. Taibi, M. Nogues, J. Aride, E. Loudghiri, A. Belayachi, Mater. Chem. Phys. 77 (2002) 912–917.
[11] H. Taguchi, J. Solid State Chem. 131 (1997) 108–114.
[12] M.R. Suchomel, C.I. Thomas, M. Allix, M.J. Rosseinsky, A.M. Fogg, Appl. Phys. Lett. 90 (2007) 112909.
[13] M. Azuma, K. Takata, T. Saito, S. Ishiwata, Y. Shimakawa, M. Takano, J. Am. Chem. Soc. 127 (2005) 8889–8892.
[14] K. Ueda, H. Tabata, T. Kawai, Science 280 (1998) 1064–1066.
[15] S.H. Feng, R.R. Xu, Acc. Chem. Res. 34 (2001) 239–247.
[16] S.H. Feng, H.M. Yuan, Z. Shi, Y. Chen, Y.W. Wang, K.K. Huang, C.M. Hou, J.X. Li, G.S. Pang, Y. Hou, J. Mater. Sci. 43 (2008) 2131–2137.
[17] Y. Chen, H.M. Yuan, G. Tian, G.H. Zhang, S.H. Feng, J. Solid State Chem. 180 (2007) 167–172.
[18] R. Dogra, A.C. Junqueira, R.N. Saxena, A.W. Carbonari, J. Mestnik-Filho, M. Moralles, Phys. Rev. B 63 (2001) 224104.
[19] W.J. Zheng, W.Q. Pang, G.Y. Meng, D.K. Peng, J. Mater. Chem. 9 (1999) 2833–2836.
[20] Y. Chen, H.M. Yuan, G.H. Li, G. Tian, S.H. Feng, J. Cryst. Growth 305 (2007) 242–248.
[21] J.J. Urban, L.O. Yang, M.H. Jo, D.S. Wang, H.K. Park, Nano Lett. 4 (2004) 1547–1550.
[22] W.C. Sheets, E. Mugnier, A. Barnabe, T.J. Marks, K.R. Poeppelmeier, Chem. Mater. 18 (2006) 7–20.
[23] W.J. Zheng, R.H. Liu, D.K. Peng, G.Y. Meng, Mater. Lett. 43 (2000) 19–22.
[24] MPMS Application Note 1014-210B, Quantum Design, 1997.
[25] D. Treves, J. Appl. Phys. 36 (1965) 1033–1039.
[26] A.K. Azad, A. Mellergard, S.-G. Eriksson, S.A. Ivanov, S.M. Yunus, F. Lindberg, G. Svensson, R. Mathieu, Mater. Res. Bull. 40 (2005) 1633–1644.
[27] L.B. Morales, R. Zysler, A. Caneiro, J. Solid State Chem. 181 (2008) 1824–1832.
[28] J.J. Neumeier, H. Terashita, Phys. Rev. B 70 (2004) 214435.